

# Development of Verapamil Hydrochloride-loaded Biopolymer-based Composite Electrospun Nanofibrous Mats: In vivo Evaluation of Enhanced Burn Wound Healing without Scar Formation

Hebatallah S Barakat<sup>1</sup>, May S Freag<sup>1</sup>, Sarah M Gaber<sup>1</sup>, Affaf Al Oufy<sup>2,3</sup>, Ossama Y Abdallah<sup>1</sup>

<sup>1</sup>Department of Pharmaceutics, Faculty of Pharmacy, Alexandria University, Alexandria, Egypt; <sup>2</sup>Department of Material & Manufacturing Engineering, Faculty of Engineering, Galala University, Galala, Egypt; <sup>3</sup>Department of Textile Engineering, Faculty of Engineering, Alexandria University, Alexandria, Egypt

Correspondence: Hebatallah S Barakat, Department of Pharmaceutics, Faculty of Pharmacy, Alexandria University, I Khartoum Square, Azarita, Messalla Post Office, PO Box 21521, Alexandria, Egypt, Tel +2 01002198334, Email hebarakat123@gmail.com

**Introduction:** Researchers aim for new heights in wound healing to produce wound dressings with unique features. Natural, synthetic, biodegradable, and biocompatible polymers especially in the nanoscale are being employed to support and provide efficient wound management. Economical and environmentally friendly sustainable wound management alternatives are becoming an urgent issue to meet future needs. Nanofibrous mats possess unique properties for ideal wound healing. They mimic the physical structure of the natural extracellular matrix (ECM), promote hemostasis, and gas permeation. Their interconnected nanoporosity prevents wound dehydration and microbial infiltration.

**Purpose:** To prepare and evaluate a novel verapamil HCl-loaded environmentally friendly composite, with biopolymer-based electrospun nanofibers suitable for application as wound dressings providing adequate wound healing with no scar formation.

**Methods:** Composite nanofibers were prepared by electrospinning of a blend of the natural biocompatible polymers, sodium alginate (SA) or zein (Z) together with polyvinyl alcohol (PVA). Composite nanofibers were characterized in terms of morphology, diameter, drug entrapment efficiency, and release. In vivo study of the therapeutic efficacy of verapamil HCl-loaded nanofibers on a Sprague Dawley rat model with dermal burn wound was investigated in terms of percent wound closure, and presence of scars.

**Results:** Combining PVA with SA or Z improved the electrospinnability and properties of the developed nanofibers. Verapamil HCl-loaded composite nanofibers showed good pharmaceutical attributes favorable for wound healing including, fiber diameter ~150 nm, high entrapment efficiency (~80–100%) and biphasic controlled drug release for 24 h. In vivo study demonstrated promising potentials for wound healing without scarring.

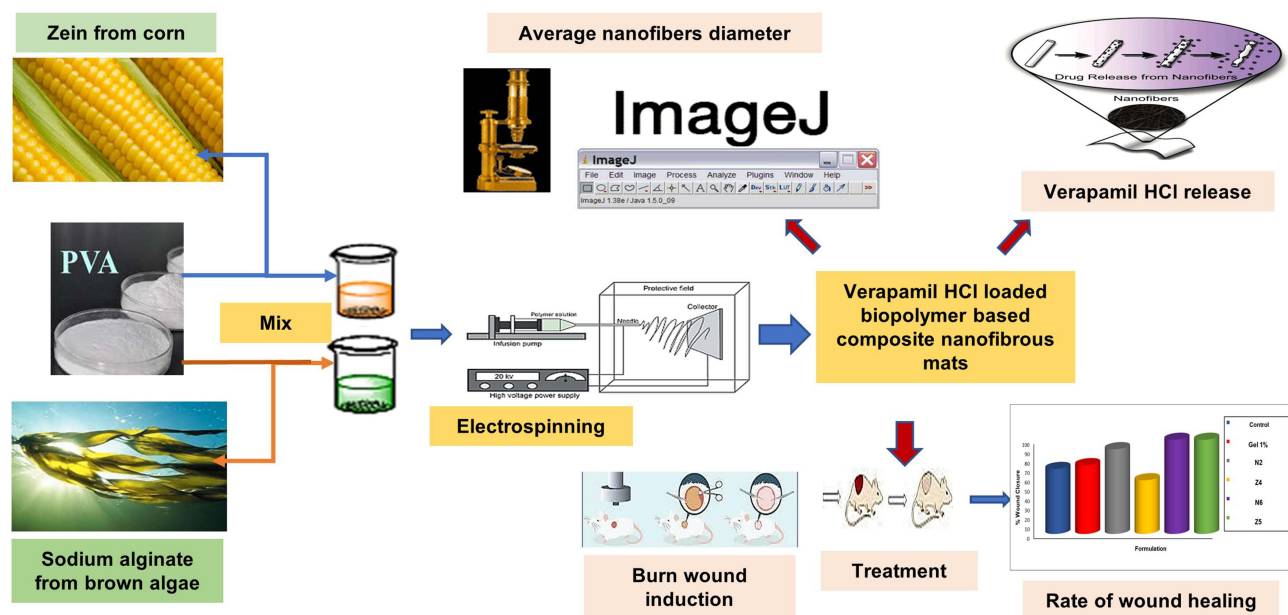
**Conclusion:** The developed nanofibrous mats combined the beneficial properties of the biopolymers and verapamil HCl to provide an increased functionality by exploiting the unique advantages of nanofibers in wound healing at a small dose proved to be insufficient in case of the conventional dosage form.

**Keywords:** wound dressing, sodium alginate, zein, nanofibers, electrospinning

## Introduction

Wound healing is a complex process mainly affected by the patient's physiological conditions, concomitant bacterial infections, and inflammation, which could delay wound closure and re-epithelialization. Diverse polymeric wound dressings have been developed to grant a favorable environment for wound healing.<sup>1</sup> Despite the large variety of efficient wound dressings currently available on the market or being developed, nanofibers are receiving a lot of attention in terms of research. They are appealing as drug carriers with high drug-loading capacity as well as controlled release.<sup>2,3</sup>

## Graphical Abstract



Their similarity to collagen and elastin fibers in healthy skin's extracellular matrix (ECM), allows them to support fibroblasts and keratinocytes to adhere and migrate throughout the wound bed, regenerate, and heal the damaged tissue.<sup>2</sup>

Electrospinning is a reliable technique for producing nanofibrous mats, with high surface area and porosity from a wide range of polymeric materials.<sup>4</sup> Such electrospun nanofibrous mats can be loaded with a variety of active ingredients to promote therapy, provide air exchange to the wound site, and keep the healing environment moist. Electrospun nanofibers can also be personalized to further enhance the fit to the wound site, providing suitable clinical coverage of wound.<sup>5</sup> Different combinations of polymers with loaded active ingredients can be developed to fulfill an unlimited number of applications. Yet, the properties of the produced nanofibers can be fine-tuned by optimizing solution properties to provide optimum chain entanglement while avoiding solution breakup as the electrified jet moves toward the collector.<sup>6</sup> Nanofibers with different three-dimensional architecture can be produced simply by changing the spinneret structures (coaxial, side-by-side, triaxial, etc) to allow for different drug release patterns.<sup>7</sup> Coaxial electrospinning is the modified version of conventional electrospinning, where it employs a coaxial needle to electrospin two polymers without being mixed. It enables the production of core-shell or multilayered nanofibers in one step.<sup>8</sup> Side-by-side electrospinning is a simple and reliable way to produce Janus nanofibers, promising for tailoring nanodrug delivery, by which synergistic action of multiple components can be achieved.<sup>9</sup> Triaxial electrospinning can solve the problem of limited drug solubility, protect the drug from surrounding environment, and control drug release kinetics, with the possibility of loading various drugs.<sup>10</sup> Layers of triaxially electrospun fibers can be loaded with different drugs to develop multidrug delivery.<sup>11</sup>

Biopolymers play an important role in drug delivery and wound dressings owing to their distinctive properties, such as biodegradability, biocompatibility, renewability, abundant availability, and inexpensiveness.<sup>12</sup> Unlike synthetic polymers, they do not require the use of hazardous organic solvents, improve drug stability, activity, as well as safety during manufacture and application on the skin.<sup>13</sup>

Sodium alginate (SA) is a polysaccharide biopolymer of marine origin. It has high water-absorbing ability 200–300 times of its weight. So it effectively absorbs wound exudates and can provide a moist environment suitable for rapid granulation and re-epithelialization and minimize bacterial infection at wound site.<sup>14</sup> Therefore, it has been particularly attractive in the biomedical field and wound healing applications in different forms as liquid, powder, compact solid, and

gel but not nanofibers in a pure form. This is because SA is a rigid, linear polysaccharide with covalently linked monomeric acid residues. Such rigid linear confirmation and the polyelectrolytic character of alginate solutions have been the main reasons behind their limited electrospinnability.<sup>15,16</sup> Furthermore, the high surface tension, absence of chain entanglements, and gelation at low concentrations, also contribute to their poor spinnability.<sup>16</sup> Attempts such as blending with hydrophilic polymers, using cosolvent systems, or modifying the alginate structure were adopted to enhance the spinnability of SA.<sup>17–19</sup> However, blending with hydrophilic polymers (eg, polyvinyl alcohol (PVA), polyethylene oxide (PEO), etc) has been found to be the most suitable method for successfully fabricating bead-free fibers. Hydrophilic polymers were found to coordinate with the alginate polymer via hydrogen bonding, reducing the strong intra- and intermolecular network between the alginate chains and increasing their flexibility. This reduces the solution's surface tension, conductivity and viscosity and hence improves its electrospinnability.<sup>17,18,20</sup>

Zein (Z) is a protein biopolymer from plant origin; widely used in many drug delivery systems including nanofibers.<sup>21</sup> Its self-assembling ability and water insolubility have made it appealing for applications such as surface protection and tissue engineering.<sup>22</sup> In wound healing, zein has largely been used as films<sup>23</sup> or electrospun nanofibrous scaffolds.<sup>24</sup> The solubility in aqueous ethanol and the self-assembling nature of zein, allowed its electrospinning without using hazardous solvents or cross-linkers.<sup>25,26</sup> However, aqueous ethanol is not an ideal solvent for electrospinning zein. Because of its high evaporation rate, it causes needle clogging, formation of ribbon-shaped fibers with poor mechanical stability, and loss of their porous structure upon contact with water.<sup>27,28</sup> This can be solved by cross-linking with UV light after electrospinning, coaxial electrospinning with polyethylene oxide (PEO) as a shell solution or blending with synthetic polymers such as PVA during electrospinning.<sup>27,29</sup>

Drug repurposing has grown to exploit the established knowledge on approved marketed drugs to employ them at their full therapeutic potentials for developing new therapies with minimal financial burden.<sup>30,31</sup> This explains why pharmaceutical companies are increasingly interested in drug repurposing where in recent years, the success rate of drug repurposing approach accounted for approximately 30% of the newly FDA approved drugs, and vaccines.<sup>32</sup>

Verapamil HCl is a calcium-channel antagonist reviewed to exert inhibitory effect on synthesis and secretion of components of extracellular matrix (ECM). Thus, it is repurposed for treating hypertrophic scars and keloids in the postoperative period as it can rebalance the biosynthesis of the extracellular matrix. It considerably increases rate of wound closure, fibroblast population in the dermis and the volume density of collagen bundles leading to higher revascularization at the injury site. Intralesional injections of verapamil HCl have been successful in treating disorders characterized by overproduction of fibrous tissue with no adverse reactions to the patients.<sup>33</sup>

Integrating all these treatment approaches appears particularly promising to achieve improved in vivo wound reparative events via a sustainable, economical, and environmentally friendly wound management approach. Although the combination of PVA with SA to improve its electrospinnability and with Z to improve the mechanical endurance of the formed nanofibers is present in literature, to the best knowledge of the authors, the literature does not offer information on the beneficial local effects of verapamil HCl as nanofibrous mats for wound healing and prevention of scar formation as well. Therefore, the present study aims to develop novel environmentally friendly verapamil HCl-loaded composite PVA-SA and PVA-Z electrospun nanofibrous mats loaded with the maximum possible amount of the drug and the biopolymers, suitable for the application as wound dressings, and capable of providing simultaneous locally controlled drug delivery for adequate wound healing with no scar formation.

## Materials and Methods

Verapamil HCl (gift from Pharaonia Pharmaceuticals, Cairo, Egypt). Sodium alginate (600 cps) (purchased from Hang Zhou Qing Technology Co., Ltd, China), Zein (Z) from maize (Sigma Aldrich grade Z3625; St Louis, MO, USA) was used as received without further purification polyvinyl alcohol (PVA) (Mwt = 205000 gm/mol) (gift from El Pharaonia pharmaceutical Co. Egypt). Ethyl alcohol of 100% purity was purchased from El-Gomhouria Company, (Alexandria, Egypt). All other chemicals were of analytical grade and used without further purification.

## Optimization of Placebo and Drug-loaded Composite Nanofibers

Composite nanofibrous mats (PVA-SA& PVA-Z) were prepared by electrospinning of a blend of the natural, biocompatible biopolymers sodium alginate (SA) or zein (Z) together with polyvinyl alcohol (PVA). Based on preliminary studies on PVA alone; 9% w/v PVA was found an optimum content for subsequent composite nanofiber formulations.

For PVA-SA composite nanofibers, three placebo composite nanofibers formulations with three different SA w/w ratios (8–12% of total polymer; N1–N3, respectively) were prepared. PVA-SA blends were prepared by first dispersing an accurately weighed amount of PVA powder using an analytical balance (Sartorius, Germany) in hot deionized water (60°C) using a magnetic stirrer (Wise stir, DAIHAN-scientific Co., Ltd, Seoul, Korea) at 60°C. Solution was then allowed to cool to 40°C, SA was then added and mixed at 40°C. Placebo nanofibers of pure PVA 9% alone (N0) were prepared for comparison.

For drug-loaded PVA-SA composite nanofibers, three drug-loaded composite nanofibers formulations with three different verapamil HCl w/w ratios (2–4% of total polymer; N4–N6, respectively) were prepared. Higher drug loading was not achievable due to drug precipitation in the polymer solution. Verapamil HCl was accurately weighed and dissolved in deionized water at room temperature. Instead of using deionized water, clear, homogeneous polymer blends for electrospinning were created in the prepared drug solution as described above. The three different drug concentrations (2–4%) were compared in terms of ease of electrospinnability, nanofiber yield, morphology, and diameter.

For PVA-Z composite nanofibers, owing to the poor water solubility of zein; the electrospinning solution was prepared in 70% (v/v) ethanol. To select the best placebo formulation for subsequent drug loading, four formulations with four different Zein w/w ratios (25–50% of total polymer concentration; Z1–Z4 respectively) were prepared.

PVA was first dissolved in 70% aqueous ethanol solution heated to 60°C with magnetic stirring until the polymer was completely dissolved. After cooling to room temperature, zein was added to the clear PVA alcoholic solution and stirred until complete solubility and homogeneity were achieved.

Three drug-loaded PVA-Z composite nanofiber formulations with three different verapamil HCl w/w ratios (2–4%; Z5–Z7, respectively) were prepared for drug-loaded PVA-Z composite nanofibers. Due to drug precipitation in the polymer solution, higher drug loads could not be obtained.

Verapamil HCl was accurately weighed and dissolved in 70% ethanol at room temperature. Polymers for electrospinning were prepared as mentioned above by dissolving the polymers in the prepared drug hydroalcoholic solution. The three different drug loads (2–4% of total polymer) were compared in terms of ease of electrospinnability, nanofiber yield, morphology, and diameter.

For electrospinning, a horizontal electrospinning station consisting of a direct current, high voltage power supply; (24 ±2 kV (Spellman High Voltage Electronics Corporation model CZE1000R, Hauppauge, New York, NY, USA) was used. A 5 mL plastic syringe was equipped with a 16-gauge stainless steel needle (spinneret) with a flat blunt end and an inner diameter of 0.9 mm. The feed rate for the polymer solution was adjusted by a syringe pump (NE1000 – Single Syringe Pump, New Era, Farmingdale, New York, NY, USA) to a constant rate of 3 mL/h. A ground collector was placed at 18 cm from the needle tip. Processing conditions and electrospinning parameters were fixed for all experiments. The electrospinning process was performed at ambient temperature of 25°C and relative humidity of <65%.

## In vitro Characterization of Composite Nanofibers

### Nanofiber Morphology and Mean Diameter

Scanning Electron Microscope; SEM (JEOL-5300, Japan) was used to examine the morphology of placebo and verapamil HCl-loaded composite (PVA-SA & PVA-Z) nanofibers. Nanofiber specimens were mounted on aluminum stubs and then were gold sputtered (JEOJEC-1100, Japan) for microscopical examination. An image analysis software (ImageJ) was then applied on representative micrographs to measure the nanofiber diameters. The average nanofiber diameters and diameter distribution were calculated using approximately 120 random segments from representative micrographs.

### Fourier Transform Infrared Spectroscopy (FTIR)

FTIR spectrometer (Shimadzu® 8400S, Kyoto, Japan) was used to record the spectra for verapamil HCl, SA, Z, PVA, placebo and drug loaded composite nanofibers. A nanofiber sample (2–4 mg) was used to form a thin film covering the diamond window of the device. Spectra were measured at spectral resolution of 2 cm<sup>-1</sup> with an average of 20 scans.



## Determination of Percent of Drug Incorporation Efficiency

Verapamil HCl content of drug-loaded mats was determined by spectrophotometric method. Nanofibrous mats were sectioned into (2×2 cm) squares. Squares were weighed and dissolved in distilled water for PVA-SA nanofibers or 70% ethanol for PVA-Z nanofibers at 50° C. Samples (1 mL) were filtered and verapamil HCl concentration was determined spectrophotometrically at  $\lambda$  max 278 nm<sup>34</sup> using UV-visible spectrophotometer (UV-1800 Shimadzu Co., Kyoto, Japan). Measurements were performed in triplicate.

The incorporation efficiency was determined by using the following equation:

$$\text{Incorporation efficiency \%} = \frac{\text{Amount of drug in nanofibers}}{\text{Theoretical drug amount}} \times 100$$

## In vitro Drug Release

The in vitro release of verapamil HCl from drug-loaded nanofibers was studied at 32°C in phosphate buffered saline (PBS) pH 7.4 to mimic the pH of wound exudate. A membraneless release method was used. Verapamil HCl-loaded electrospun nanofibrous mats were sectioned into 2×2 cm squares. Owing to possible nonuniformity in the thickness of nanofibrous fragments; they were weighed to assure having identical polymer and drug content. Fragments were then folded to mimic the actual way of in vivo application and placed in round stainless-steel cups (16 mm width and 3 mm depth) to be held in place at the bottom of 50 mL capped bottles containing 20 mL of the release medium. Sink conditions prevailed based on drug solubility data. Bottles were shaken in a thermostatically controlled shaking water bath at 32°C for 12 h at 60 rpm. At predetermined time intervals (1, 2, 4, 6, 8, 10, and 12 h) 2 mL-samples of the release medium were withdrawn and replaced with the same volume of fresh medium pre-equilibrated at 32°C. The concentration of released verapamil HCl was determined spectrophotometrically at  $\lambda$  max 278 nm<sup>34</sup> after correction for dilution. All measurements were performed in triplicate.

## In vivo Studies

### Animals

Female Sprague Dawley rats weighing between 210 and 250 g were purchased from the animal house of Pharos University, Alexandria, Egypt. Rats were kept under standard laboratory conditions and veterinary supervision with no restrictions on water and food. Eighteen female rats were randomly separated into six groups of three rats. Rats were housed in individual cages and kept in a temperature-controlled room at 20–25°C on a 12 h light/12 h dark cycle. They were provided with water and standard meals. Experimental protocol was approved by Institutional Animal Care and Use Committee, Faculty of Pharmacy, Alexandria University, Alexandria, Egypt (AU06202211261136).

### Burn Wound Induction

Just before inflicting the burn, rats were anesthetized using diethyl ether. Each rat's back hair was shaved to get smooth, hairless skin. The shaved back skin of anesthetized animals was exposed to hot rods to form the burn wound. For this procedure, a cylindrical stainless steel rod (radius 10 mm) was placed in hot water (100°C) for 1 min and then on the back of rats and held for 20 s. After forming standard, second-degree burns, they were covered for two days with cotton and gauze pre-wetted with saline before being removed to form a remarkable wound.<sup>35</sup> Each rat was subjected to four burns.

### Treatment Groups

Six groups of rats were formed at random (each of three rats with a total of 12 wounds) according to the treatment applied on the formed wounds. Owing to possible nonuniformity in the thickness of nanofibrous fragments; they were weighed prior to any application to assure having identical polymer and drug content. Wounds were either treated with verapamil HCl gel (1% in HPMC 1.5% w/v) (dose equivalent to 0.5 mg verapamil HCl), placebo PVA-SA composite nanofibers (N2), verapamil HCl loaded PVA-SA composite nanofibers (N6) (dose equivalent to 0.5 mg verapamil HCl),

placebo PVA-Z composite nanofibers (Z4), verapamil HCl loaded PVA-Z composite nanofibers (Z5) (dose equivalent to 0.5 mg verapamil HCl) and finally a control untreated group. Each rat, as mentioned previously, was subjected to four wounds, and was kept in a separate cage. The same formulation was applied on the four wounds in the three rats. Formulations were repeatedly applied to the wounds every day for 14 days. Nanofibrous mats were folded to fit the wound areas. They were covered with adhesive plaster to be fixed in place. Regarding the control wounds, they were cleaned daily with cotton soaked in normal saline. The wound diameters were measured and recorded on a regular basis.

## Assessment of Wound Healing

### Morphological Examination and Scar Monitoring

Wound sites were monitored visually and digitally photographed while maintaining constant optical zoom for healing, exudate, redness, hyperpigmentation, and scar formation throughout the whole study period (14 days) and after the end of treatment until day 17 post-wounding.

### Measurement of Wound Size

Progressive decrease in the wound size was periodically monitored every day prior to treatment application. The wound diameter was determined using a vernier caliper by measuring the distance between two opposite outer edges of the wound margins.<sup>36</sup> Two measurements approximately 90° apart were taken with the largest distance has been considered as one of them. Wounds were digitally photographed on 0.3, 5, 7, 9, 11, and 14 days post-wounding while maintaining constant optical zoom.

### Calculation of Wound Closure Percent (Efficacy Indices)

Wound contraction is a crucial feature in the healing process which helps to close the wound by decreasing the gap between its dermal edges and reducing wound surface area. It mainly depends on the repairing ability of tissues. It was determined at days 3, 5, 7, 9, 11, and 14 from the beginning of treatment.<sup>36</sup>

The wound contraction rate was measured as percentage reduction in the wound size (% efficacy indices; % EI). The % EI of the wound size was calculated by the following equation:

$$\% EI = \frac{\text{Initial wound diameter} - \text{wound diameter in } N^{\text{th}} \text{ day}}{\text{Initial wound diameter}} * 100$$

### Histological Examination

At the end of treatment, full thickness skin biopsies of wounds with surrounding tissues were collected. Histological examination was performed for wounds treated with different treatments, control untreated wounds as well as normal skin for further comparison. Specimens were fixed in 10% formaldehyde, embedded in paraffin, cut into 5 µm pieces, and stained with hematoxylin and eosin (H&E). Sections were visualized under a light microscope at 50× and 500×. The degree of epithelization, the presence or absence of inflammatory cells, the nature of collagen and fibrous tissue were all examined in different fields.<sup>37</sup>

## Statistical Analysis

The in vitro data was coded using R program. The variables were expressed as mean ±SD. Permutation test using library (“coin”) was used to detect any statistically significant difference between groups.<sup>38</sup> Statistical significance was considered when  $p < 0.05$ . Regarding in vivo studies, the collected data was wrangled, coded, and analyzed using SPSS v 25.0 software (IBM Corporation, Armonk, NY, USA). The variables were expressed as mean ±SD. One-way ANOVA with bootstrapping was used to detect any statistically significant difference between groups. Pairwise comparison was done using Tukey’s test. Statistical significance was considered when  $p < 0.05$ .

## Results

The current work aimed at the reproducible production and clinical evaluation of novel biopolymer based environmentally friendly verapamil HCl-loaded composite electrospun nanofibrous mats. The target was to employ the maximum

possible load of biopolymers (owing to their great value in wound healing) as well as the repurposed drug (verapamil HCl), without interfering with the initiation or the continuation of the electrospinning process. Therefore, optimization was based on gradient increase of polymers and drug loads. Selection criteria were based on the reproducibility and continuity of the electrospinning process, yield of the formed fibers, ease of handling, and the morphology of the produced fibrous mats as revealed by their SEM images. Based on those criteria only the promising formulations were selected for the subsequent characterization.

## Optimization of Composite Nanofibers

In the preliminary trials, electrospinning of PVA 9% w/v solution (N0) resulted in a good yield of easily handled nanofibers with suitable manageability (Figure 1a). Also, PVA 9% w/v solution (N0) could allow SA or Z to be incorporated in the blend without forming a very thick solution difficult to electrospin. Therefore, it was selected as the optimum concentration of PVA suitable for blending with SA and Z throughout the study. Subsequent weight ratios of SA, Z, and verapamil HCl were calculated relative to the total polymer weights.

## Composite PVA-SA Nanofibers

Electrospinning of PVA-SA polymer blend with SA weight ratio 10% (N2) produced a good yield of smooth nanofibers with suitable manageability, ease of handling and removal from the aluminum foil (Figure 1b). Higher concentration of

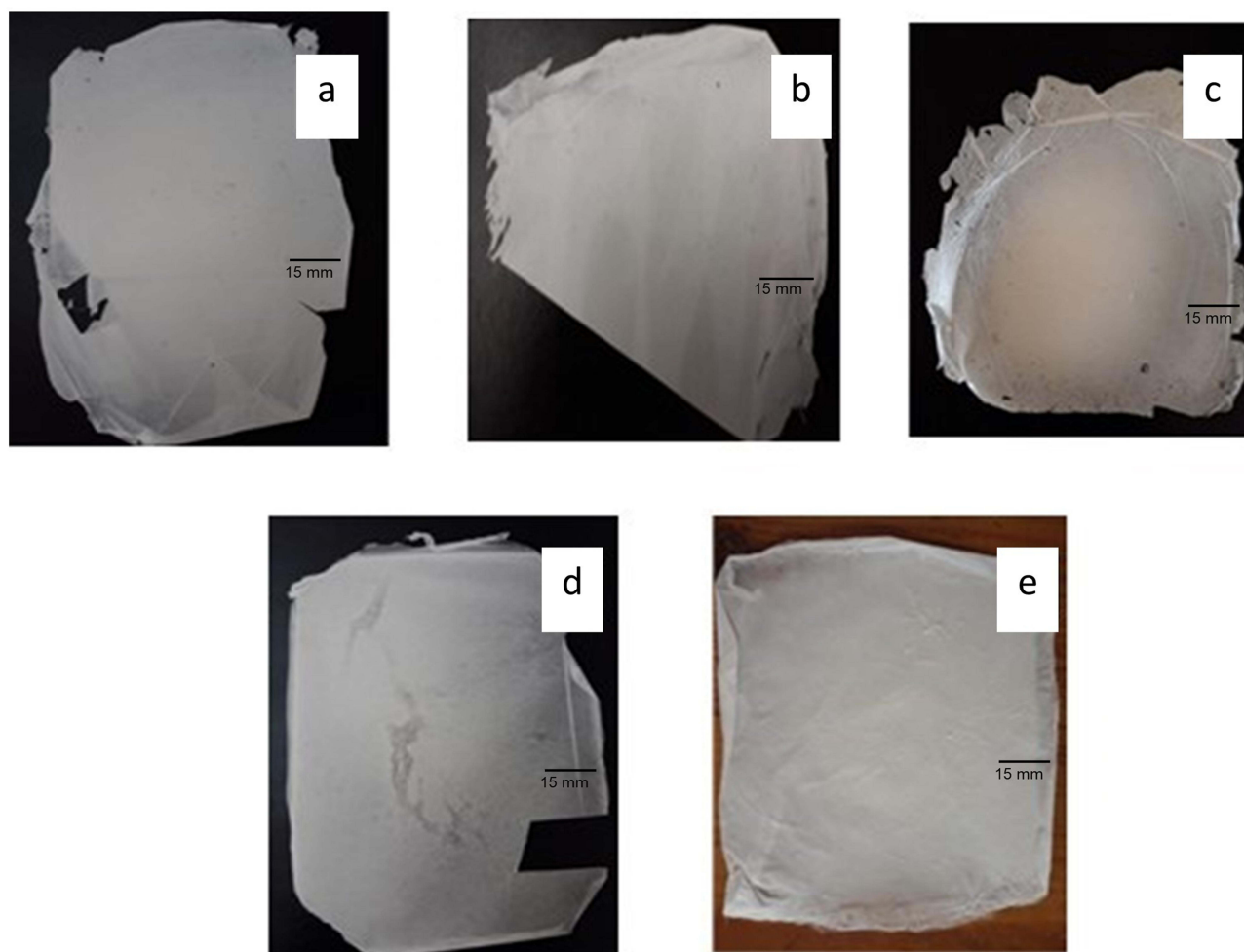


**Figure 1** Photographs of different composite nanofibrous mats; (a) PVA 9% (N0), (b) placebo PVA-SA 10% composite nanofibers (N2), (c) verapamil HCl-loaded composite nanofibrous mats. PVA-SA-verapamil HCl 10/4% (N6), (d) placebo PVA-Z (25%) composite nanofibers (Z4), and (e) verapamil HCl loaded composite nanofibrous mats PVA-Z-verapamil HCl (25/2%) (Z5).

SA in the polymer blend (N3) hindered electrospinning possibly owing to altered solution properties. Therefore, it was concluded that PVA-SA 10% w/w (N2) blend was the most optimum placebo nanofiber formulation suitable for subsequent drug loading.

PVA-SA 10% solutions containing 2–4%, verapamil HCl were all found to be clear and homogeneous with no apparent precipitation. As the drug load was increased, the electrospinnability and quality of the produced nanofibers improved. The 4% verapamil HCl loaded PVA-SA blend (N6) produced the highest yield of nanofibers, resulting in the best drug loaded fibers in terms of quantity, ease of handling, and manageability as shown in [Figure 1c](#). Therefore, the nanofiber formulations (N2 and N6) were selected for further characterization.

## Composite PVA-Z Nanofibers

Results revealed that under the selected optimized electrospinning conditions the polymer blend containing the highest zein weight ratio of 50% w/w (Z1) suffered from clogging during electrospinning and consequently a decrease in the process productivity and the product quality.

However, when the mass ratio of zein in the polymer blend was reduced to 25% in (Z4); electrospinning improved in a manner allowing good nanofibrous mat formation. Therefore, placebo blend containing zein weight ratio of 25% (Z4) were considered acceptable placebo nanofibrous mats ([Figure 1d](#)) suitable for subsequent drug loading.

Verapamil HCl in concentrations 2–4% (Z5–Z7, respectively) were combined with (Z4) to fabricate drug loaded composite PVA-Z nonfibrous mats. In contrast to verapamil HCl-loaded composite PVA-SA nanofibers, presence of lower verapamil HCl content (2%) greatly improved the quality and quantity of fibers. Verapamil HCl-loaded PVA-Z nanofibrous mats at zein weight ratio of 25% loaded with 2% verapamil HCl (Z5) ([Figure 1e](#)) were optimum and therefore (Z4 and Z5) were selected for further characterization.

## Characterization of Composite Nanofibers

Characterization of nanofibers can be performed via several in vitro and in vivo studies. However, the exact characterization criteria selected for this manuscript were based on the intended application, behavior when in contact with site of application, and the expected mechanism of action.

## SEM Analysis

SEM was used to examine and compare the morphological structure of the placebo PVA-SA and PVA-Z composite nanofibers formulations (N2) and (Z4), as well as the drug-loaded formulations (N6) and (Z5) compared with that of pure PVA (N0). Continuous, uniform nanofibers were obtained from all formulations. However, SA, Z, and verapamil HCl were found to play a role in fiber morphology and diameter as depicted in the SEM micrographs shown in [Figure 2](#). For pure PVA (N0), the fibers obtained were uniform and continuous with few beads ([Figure 2a](#)) and average diameter of approximately 105 nm. For PVA-SA composite placebo nanofibers (N2); continuous, uniform relatively larger, but still beaded fibers were obtained ([Figure 2b](#)). The average diameter increased compared to pure PVA nanofibers reaching 154 nm. SEM images of the verapamil HCl-loaded electrospun PVA-SA composite nanofibers (N6) revealed almost bead-free nanofibers with no drug particles on fiber surfaces indicating no drug precipitation during the electrospinning process ([Figure 2c](#)). The average mean diameter of the drug-loaded nanofibers was approximately 156 nm indicating that entrapment of verapamil HCl in the nanofibers had no effect on their diameter.

For placebo PVA-Z composite nanofibrous mats (Z4) it was revealed that zein played a major role in nanofiber morphology. SEM micrographs revealed uniform interconnected bead-free random nanofibrous structures along their lengths ([Figure 2d](#)) with larger average diameter of approximately 172 nm compared to pure PVA solution (N0) ([Figure 2a](#)).

For verapamil HCl-loaded PVA-Z composite nanofibrous mats it was worth noting that there were no drug aggregates on the fiber surface, implying no phase separation during electrospinning ([Figure 2e](#)). In contrast to PVA-SA composite nanofibers; slight decrease in the average diameter of the composite nanofibers PVA-Z with the inclusion of verapamil HCl (149 nm) relative to the placebo nanofibers (172 nm) was observed. Therefore, it is crucial to highlight that the drug influence on fiber diameter varies depending on the polymer blend and solvent used. [Figure 3](#) shows nanofiber diameter distribution curves of PVA (N0), composite (PVA-Z; Z4 and Z5) and (PVA-SA; N2 and N6) nanofiber formulations



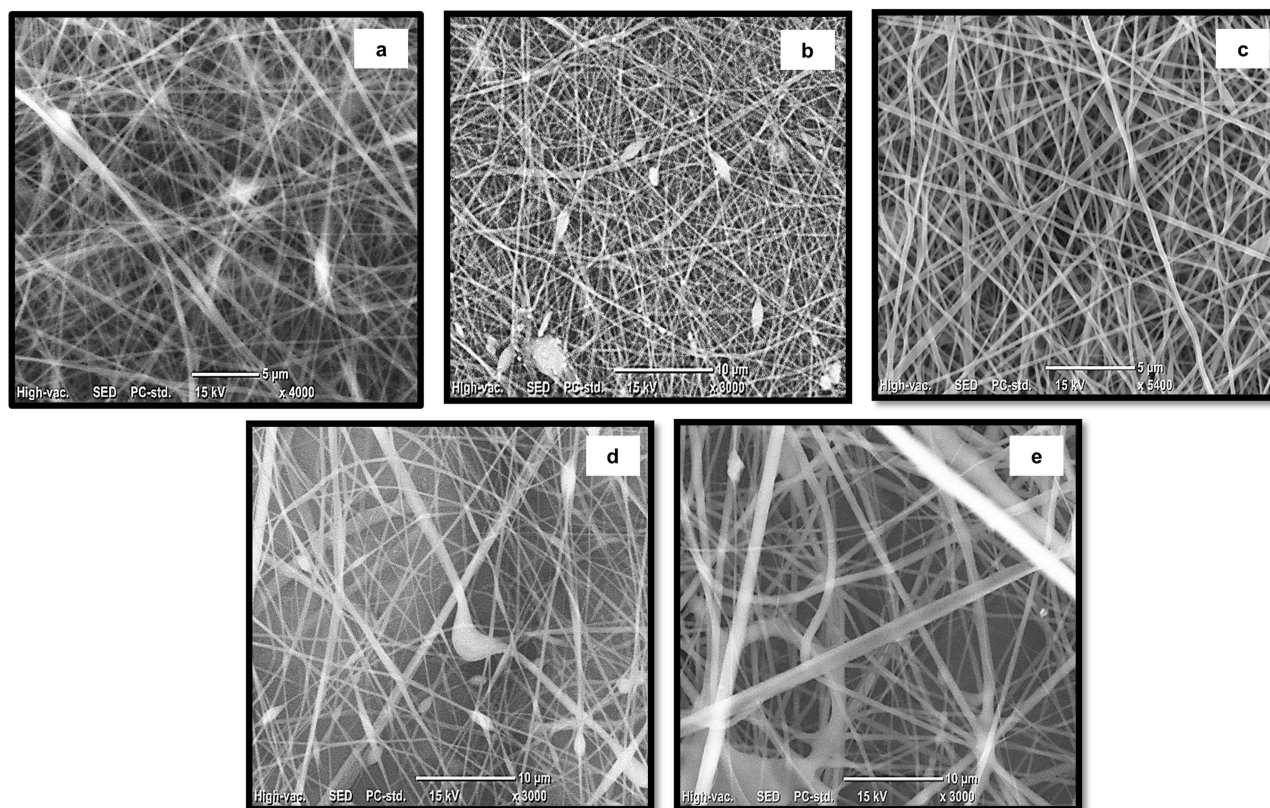


**Figure 2** SEM micrographs of (a) pure PVA 9% (N0), (b) placebo PVA-SA 10% (N2), (c) verapamil HCl loaded PVA-SA-verapamil 10.4% (N6), (d) placebo PVA-Z 25% (Z4), and (e) verapamil HCl-loaded PVA-Z-verapamil 25, 2% (Z5).

measured using (ImageJ) analysis software from approximately 120 random measurements for each sample using representative micrographs.

## Fourier Transform Infrared Spectroscopy (FTIR)

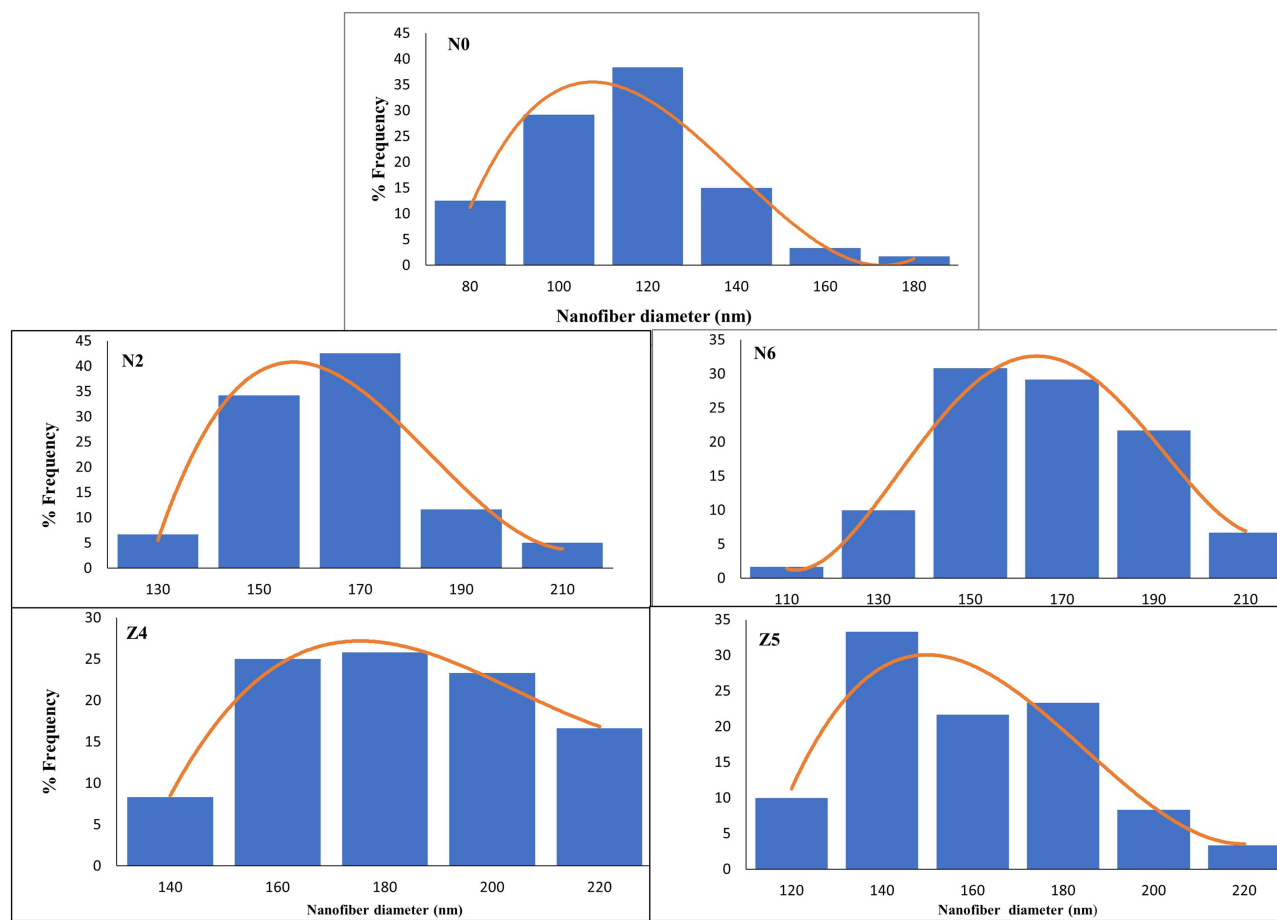
Fourier transform infrared spectroscopy (FTIR) has been used to detect any interactions between blended polymers as well as between the drug and the polymers.

Figure 4 shows the various peaks corresponding to the various functional groups of pure PVA such as CH<sub>2</sub> groups at 2941 cm<sup>-1</sup>, C-O group at 1085 cm<sup>-1</sup>, 1734 cm<sup>-1</sup> (residual acetyl groups), and OH stretching at 3369 cm<sup>-1</sup>. SA showed a peak at 3292 cm<sup>-1</sup> for OH groups. Asymmetric and symmetric COO group peaks corresponded to wave number of 1583 cm<sup>-1</sup> and 1405 cm<sup>-1</sup> respectively.

Pure verapamil HCl displayed characteristic peaks at 2956 and 2839 cm<sup>-1</sup> for C-H stretching vibrations in methyl, at 2580 and 2536 cm<sup>-1</sup> for aldehydic C-H stretching vibrations, 2237 cm<sup>-1</sup> for C≡N stretching vibrations, 1592 for C=C in aromatic ring, 1256 and 1141 for C-O stretching, 1020 cm<sup>-1</sup> for C-N aliphatic stretching vibrations and 816 cm<sup>-1</sup> (meta substituted benzene).

The FTIR spectra of blended polymers revealed spectral characteristics similar to those for the individual polymers, but with some bands shifted from their original positions. As shown in Figure 4, spectra of PVA-SA composite nanofibers (N2) showed prominent peaks at 3443 cm<sup>-1</sup> of the hydroxyl group, peak at 2942 cm<sup>-1</sup> of CH stretching and peak at 1648 cm<sup>-1</sup> of (COO). The broad peak of hydroxyl group at 3443 cm<sup>-1</sup> is attributed to the hydrogen bonding between the hydroxyl groups of PVA and SA. The slight shifting of carboxylate band to higher wave number also indicated the interaction of SA with PVA through hydrogen bonding between the etheric oxygen of PVA and hydroxyl group of SA.<sup>39</sup>





**Figure 3** Nanofiber diameter distribution curves of PVA (N0) and composite (PVA-SA; N2 and N6) and (PVA-Z; Z4 and Z5) nanofiber formulations.

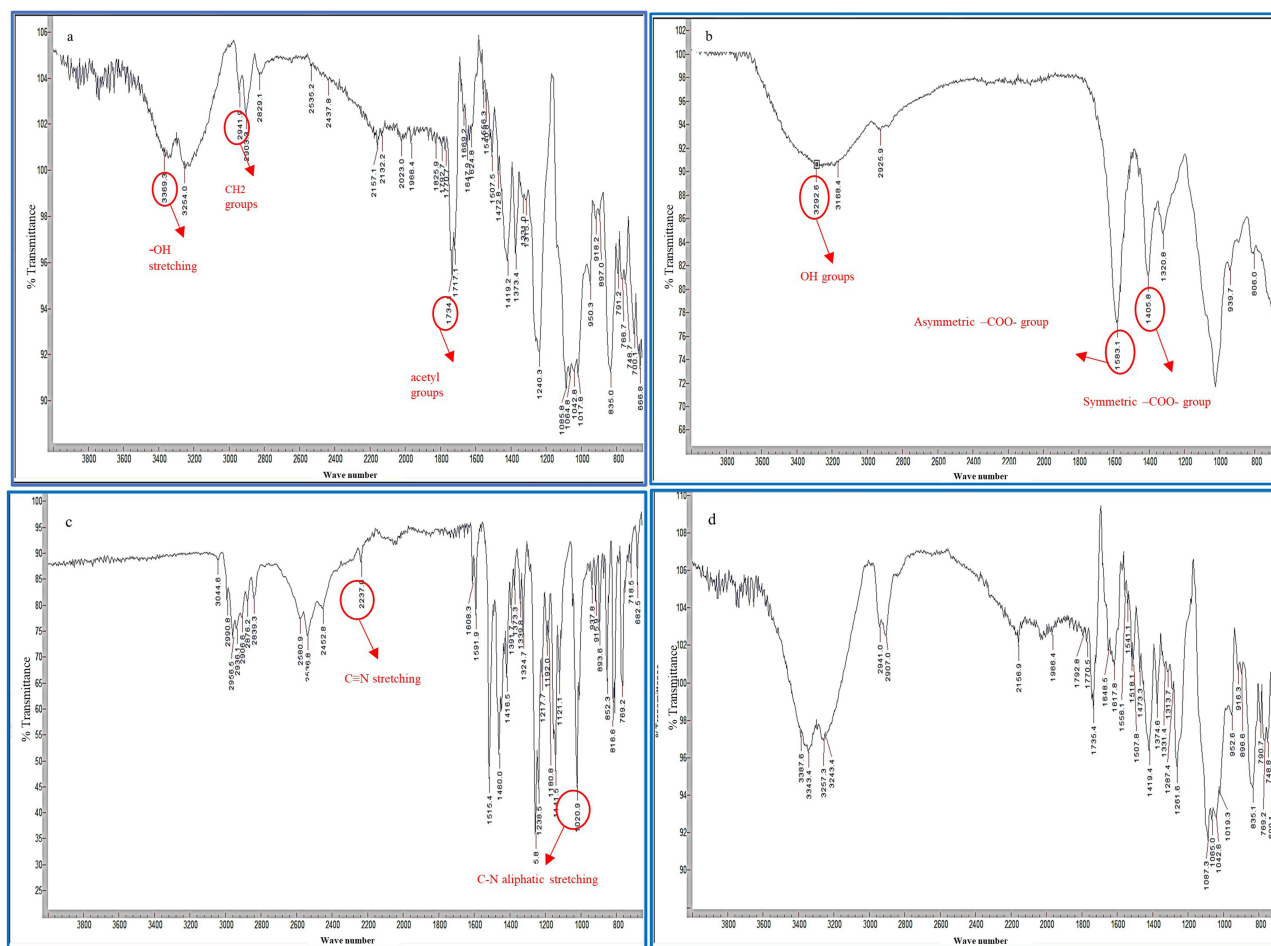
In contrast, the FTIR spectra obtained from the verapamil HCl-loaded nanofibrous mats (N6) could be simply regarded as superposition of pure drug and polymers confirming no chemical interaction between the drug and the polymers as shown in Figure 4.

Figure 5 shows the various peaks corresponding to the various functional groups of pure zein, PVA, verapamil HCl, placebo PVA-Z (Z4) and verapamil HCl-loaded PVA-Z (Z5) electrospun scaffolds. Two apparent characteristic peaks for zein were at  $3275\text{ cm}^{-1}$  (N–H stretching) and  $1741\text{ cm}^{-1}$  (C=O stretching). The presence of two obvious vibrational bands of the protein backbone; amide I and amide II were observed. The most characteristic spectral region to the protein secondary structure constituents is the amide I band ( $1636\text{ cm}^{-1}$ ), which is derived from the C=O stretch vibrations. In contrast the amide II band ( $1526\text{ cm}^{-1}$ ) is due to the C–N stretching and N–H bending for pure zein powder. The characteristic peaks observed at  $2931$  and  $2957\text{ cm}^{-1}$  were derived from C–H bands from CH<sub>2</sub> and CH<sub>3</sub> functional groups characteristic free fatty acids that exist in zein.

For placebo PVA-Z electrospun mat (Z4), the peaks were displayed at  $3270\text{ cm}^{-1}$  (N–H stretching and O–H stretching),  $1716\text{ cm}^{-1}$  (C=O stretch vibrations),  $1653\text{ cm}^{-1}$  (absorbed water), and  $1436$  and  $1507\text{ cm}^{-1}$  (C–H bending). All the characteristic peaks of PVA, zein and drug were visible in drug-loaded PVA-Z composite nanofibrous mats (Z5). Most of the peaks of verapamil HCl, PVA and Z in the PVA-Z drug-loaded nanofibers have been overlapped and shifted suggesting hydrogen bond formation and compatibility of components with no chemical interaction.

## Determination of Percent Drug Incorporation Efficiency

High entrapment efficiency of 80–100% verapamil HCl in the composite nanofibers (N6) and (Z4) was obtained.



**Figure 4** Comparative FTIR Spectra of (a) PVA, (b) SA, (c) verapamil HCl, and (d) PVA-SA-Verapamil HCl loaded nanofibers (N6).

## In vitro Drug Release Studies

Being a weak base verapamil HCl exhibits pH dependent solubility. Although it is freely soluble in water and at low pH values, it is only slightly soluble at neutral pH. Its saturated solubility in PBS pH 7.4 was found to be ~0.22 mg/mL. Drug release from verapamil HCl-loaded PVA-SA composite nanofibers (N6) and verapamil HCl-loaded PVA-Z composite nanofibers (Z5) in phosphate buffer pH 7.4 is shown in [Figure 6](#). Release profiles were typically biphasic with an initial burst release phase during the first 2 h of about 29.7% ±1.15 and 19% ±1.0 for N6 and Z5 respectively. This was followed by a slower sustained release of the drug up to 24 h. Percent release in phosphate buffer pH 7.4 for drug-loaded PVA-SA and PVA-Z was approximately 93.7% ±2.08 and 68.0%±1.0 respectively after 24 h. N6 showed significantly higher release rate than Z5 at both 2 and 24 h ( $p=0.027$  and  $p=0.026$ , respectively) ([Table S1](#) and [Figure S1](#)).

## In vivo Study

### Evaluation of Wound Healing

Treatment efficacy of verapamil HCl-loaded composite nanofibers (N6 and Z5) on a Sprague Dawley rat model with dermal burn wound was investigated in comparison with equivalent doses (0.5 mg of verapamil HCl) of conventional verapamil HCl gel 1% and placebo composite nanofibers (N2 and Z4). Percent wound closure was calculated for each group to estimate the healing efficiency of the different formulations compared with an untreated control group. Photographs of wounds and percentage wound closure on the assessment days are presented in [Figures 7](#) and [8](#), respectively.

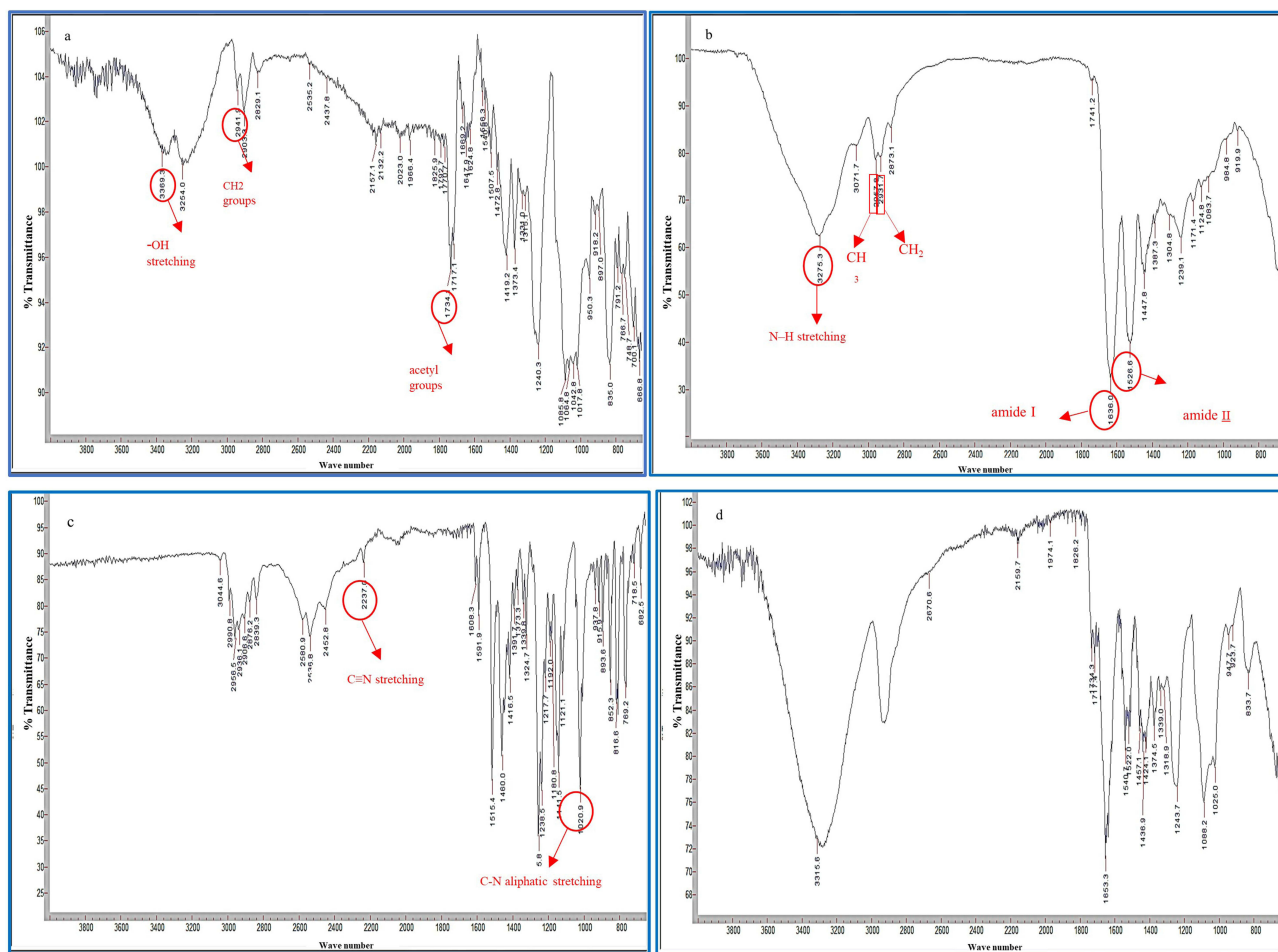


Figure 5 Comparative FTIR spectra of (a) PVA, (b) Z, (c) verapamil HCl, and (d) PVA-Z-verapamil HCl-loaded nanofibers (Z5).

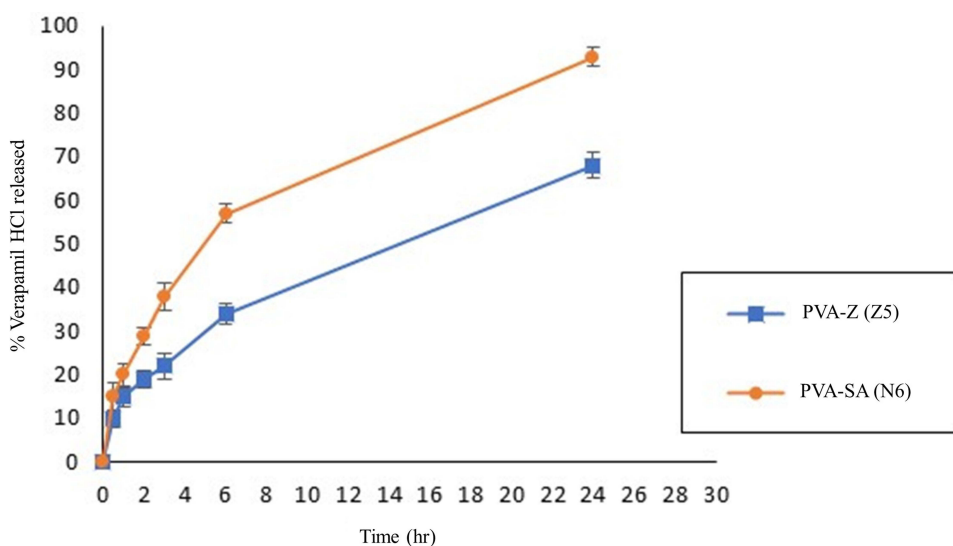
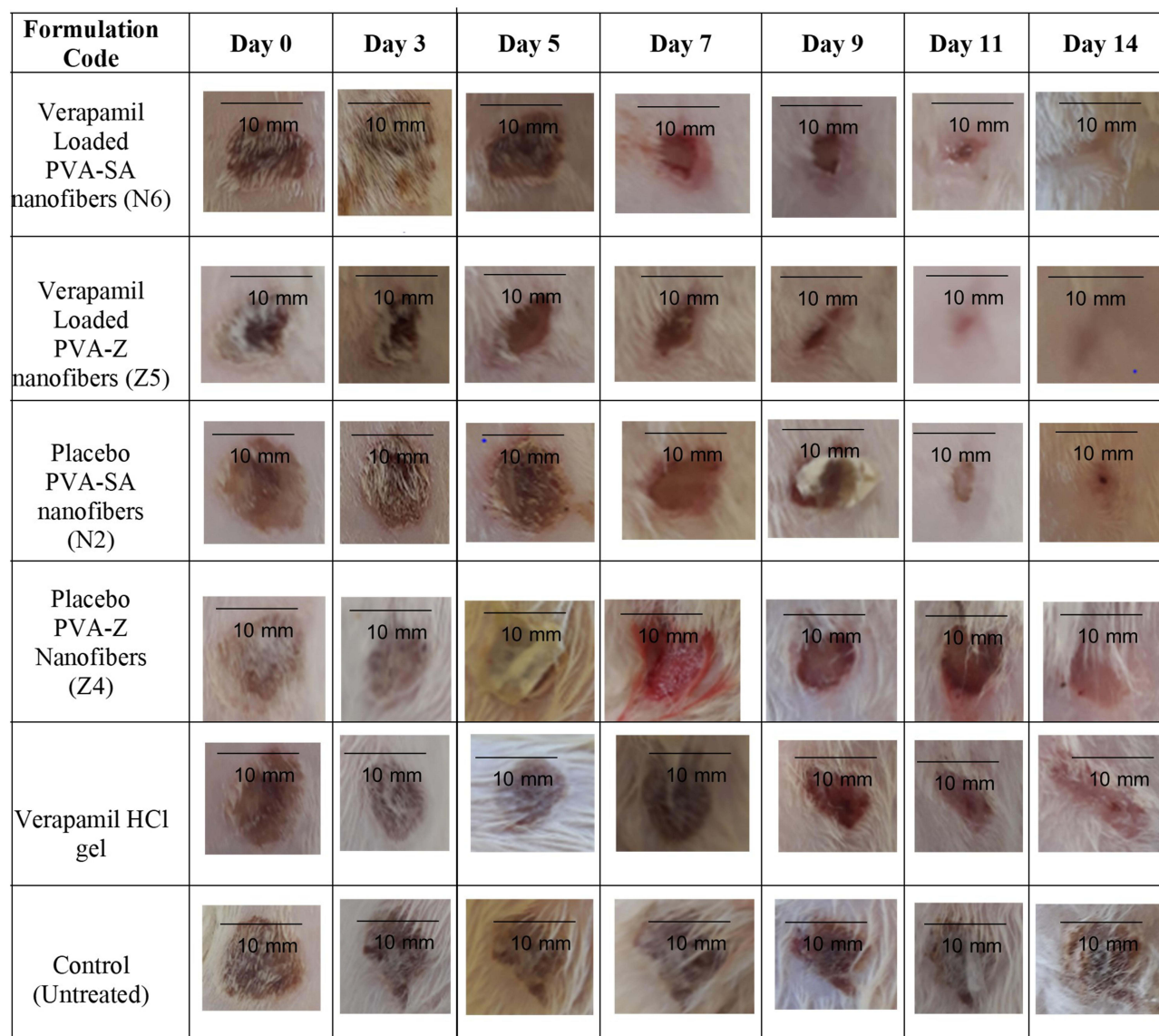


Figure 6 In vitro drug release profiles of verapamil HCl from PVA-SA (N6) and PVA-Z (Z5) composite nanofibers in phosphate buffer pH 7.4 at 32°C.



**Figure 7** Stages of wound healing of the different treatment groups.

Data indicated that the untreated control rats showed only 23%  $\pm$ 6.08 and 69%  $\pm$ 5.3 wound healing after the first and second weeks, respectively, which was significantly different from the composite nanofiber treatment groups ( $p < 0.001$ ). However, healing in the case of the conventional verapamil HCl gel group was only slightly better than the control group showing 28%  $\pm$ 3 and 73%  $\pm$ 3 wound healing after the first and second weeks, respectively. At the end of treatment, no significant difference between verapamil HCl gel and control groups was observed ( $p = 0.814$ ).

Comparing the results of the two different placebo nanofiber formulations (N2 and Z4) showed the significant superiority of PVA-SA nanofibers (N2) over PVA-Z nanofibers (Z4). After 2 weeks the percentage of wound closure of the placebo PVA-SA nanofibers was 90%  $\pm$ 5 compared to 67%  $\pm$ 2 only for placebo PVA-Z nanofibers. Comparing both placebo nanofibers and control group, showed insignificant difference of placebo PVA-Z nanofibers to control ( $p = 0.98$ ) while placebo PVA-SA (N2) nanofibers exhibited better healing rate. Placebo nanofibers (N2); produced 90%  $\pm$ 5 wound healing after 14 days. This result is considered significantly better than verapamil HCl gel (73%  $\pm$ 3) ( $p < 0.001$ ).

Both verapamil HCl-loaded PVA-SA (N6) and PVA-Z (Z5) nanofibers had a high percentage of wound closure, which was significantly different from the control and verapamil HCl gel (54%  $\pm$ 4 and 100%  $\pm$ 2 and 33%  $\pm$ 4.3 and 100%  $\pm$ 5 for N6 and Z5 after the first and second weeks, respectively) ( $p < 0.001$ ).

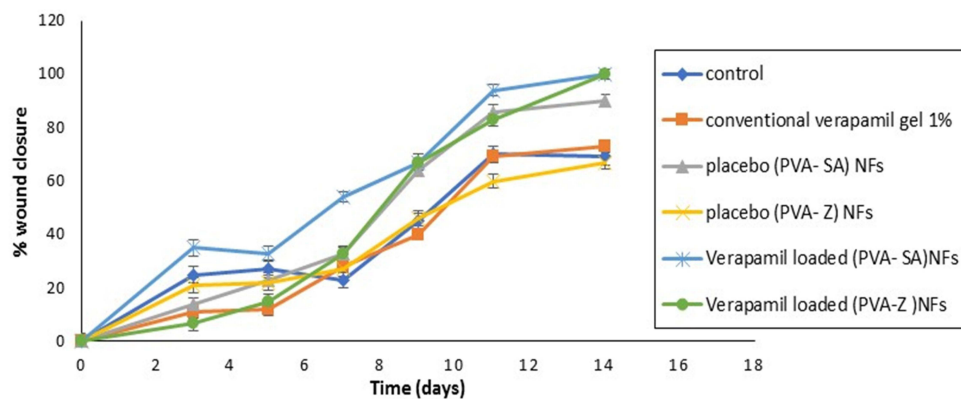


**Figure 8** Comparative wound closure percentage of different treatment groups for 14 days.

For verapamil HCl-loaded PVA-SA composite nanofibers (N6); its superior percentage of wound healing was evident during the first week of treatment where  $54\% \pm 4$  wound healing results were obtained compared to  $33\% \pm 4.3$  only for PVA-Z composite nanofibers (Z5) (Table S2 and Figure S2). Both types achieved complete healing by the end of experiment. These findings suggest that both types of verapamil HCl-loaded electrospun mats (PVA-SA and PVA-Z) are good candidates as smart wound dressings for rapid and complete wound healing.

## Scar Monitoring

In the current study, visual inspection of scars was performed until the 17th day post-wounding as a simple method to detect the presence or absence of scars. Despite the low verapamil HCl dose in the drug-loaded nanofibrous mats no scars were observed in all wounds treated with verapamil HCl-loaded composite nanofibers (N6 and Z5).

## Histopathological Examination

For additional investigation of the quality and maturity of the newly formed healed tissues of different treatment groups, full thickness sections of normal skin and treated wounds, were collected and stained with hematoxylin and eosin (H&E) for microscopical examination of skin layers in comparison with normal skin. The normal skin showed an epidermis, dermis layer, hair follicles, sebaceous gland and an areolar woven network of collagen fibers arranged in the dermal layer (Figure 9A).

Histopathological assessment of untreated control wounds on day 14 showed regeneration with incomplete strata and absence of keratin layer (Figure 9B). Wounds treated with conventional verapamil HCl gel showed enhanced stratum granulosum but with vacuolation of cells and different thickness (incomplete regeneration) (Figure 9C). Wounds treated with placebo PVA-SA (N2) nanofibrous mats also showed enhanced stratum granulosum, normal thickness with production of keratin (Figure 9D). In contrast, wounds treated with placebo PVA-Z (Z4) nanofibrous mats showed regeneration with vacuolated cells, decreased stratum granulosum and absence of keratin (Figure 9E). This result agreed with healing rate results which indicated that placebo PVA-SA (N2) had a higher percentage of wound closure than placebo PVA-Z nanofibers (Z4) and conventional verapamil HCl gel. Verapamil HCl-loaded PVA-SA nanofiber (N6) treated wounds showed significantly enhanced histological characteristics; with almost complete stratum granulosum, recovery of cells and keratinization (Figure 9F). Surprisingly, wounds treated with verapamil HCl-loaded PVA-Z (Z5) nanofibers were characterized with enhanced proliferation of cells, increased thickness, complete keratin production comparable to that of normal skin (Figure 9G).

Comparing both verapamil HCl-loaded composite nanofibers (N6 and Z5), results showed significant enhancement in histological characteristics with superiority of verapamil HCl-loaded PVA-Z nanofibers (Z5) despite its more delayed percentage of wound closure relative to verapamil HCl-loaded PVA-SA nanofibers (N6).



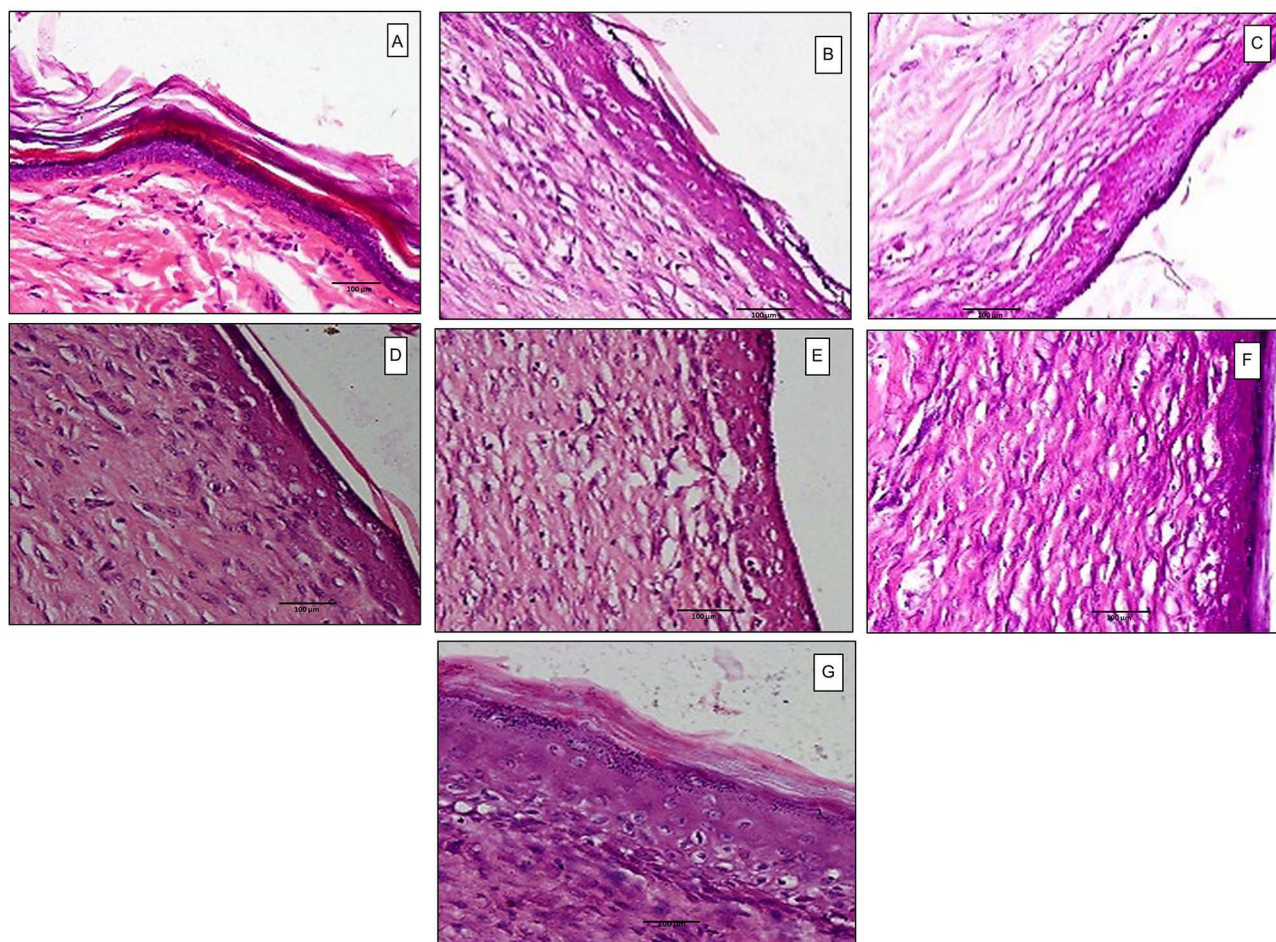


**Figure 9** Histopathological examination at 500 $\times$  magnification power of (a) normal skin, (b) control untreated group, (c) treated with verapamil HCl gel, (d) treated with placebo PVA-SA nanofibers (N2), (e) treated with placebo PVA-Z nanofibers (Z4), (f) treated with verapamil HCl-loaded PVA-SA nanofibers (N6), (g) treated with verapamil HCl-loaded PVA-Z nanofibers (Z5), on day 14 post-wounding.

## Discussion

SA is a natural marine polymer with many uses in the biomedical field in different forms but not in a pure electrospun nanofiber form owing to its rigid linear structure and polyelectrolytic character which limits its electrospinnability. The polyelectrolytic nature of SA imparts high conductivity with the ability to form solutions with a wide range of viscosities. It also causes repulsive forces among the polyanions hindering SA electrospinning. It was found that the rigid and extended worm-like molecular chains of alginate could hinder effective chain entanglements in its aqueous media. These may be the main reasons hindering the electrospinning of pure SA from its aqueous solution.<sup>15,16</sup> As a result, enhancing the flexibility and entanglements of SA chains through the addition of polyols may be important in resolving the problem.<sup>40</sup> Electrospinning of pure PVA solution, however, has been intensively explored to produce biodegradable nanofibrous mats.<sup>41</sup> Therefore, to improve the entanglement ability of the polymer chains during the electrospinning process, the flexible synthetic polymer, PVA was combined with the rigid natural polymer, SA.<sup>42</sup> Interaction through intermolecular hydrogen bonding between SA and PVA as verified by FTIR reduces the repulsive forces among polyanionic SA chains, consequently, electrospinning of PVA-SA blends could be carried out successfully.<sup>43</sup>

Zein has a hydrophobic property because of the presence of the nonpolar amino acids, glutamine and proline, as key constituents.<sup>44</sup> Electrospinning of pure zein solutions was difficult and the formed zein nanofibers were too fragile. However, addition of PVA to the spinning solution can improve both mechanical and therapeutic properties of zein and change its hydrophobic nature.<sup>44,45</sup> This is because hydrophobic/hydrophilic properties of nanofibrous scaffolds are

crucial parameters that can greatly influence cell adhesion and proliferation.<sup>46</sup> Thus, PVA was combined with the natural polymer zein to form composite nanofibers with enhanced characteristics.

High zein content interfered with electrospinning and decreased the process productivity. This could be attributed to ethanol's volatility, which causes a rapid increase in the viscosity of the concentrated zein solution on the surface of the droplet.<sup>27</sup> A similar observation was obtained by Wang and Mousavi<sup>47</sup> who fabricated lidocaine-loaded zein fibers. During the electrospinning process, solvent evaporation took place. Accordingly, concentration on the surface of the droplet increases. The higher the solution concentration, the higher the viscosity. If the viscosity becomes too high, the applied electrical force would not be sufficient to overcome the force of viscous drag at the air-droplet interface, causing clogging of the needle tip.

Success of the electrospinning process can also be reflected via fiber morphology. Presence of beads (which are defined as nonevaporated solvent zones) in the fibers are indicative of unstable process, leading to low reproducibility of the obtained material. It occurs due to insufficient stretching of the polymer solution during fiber formation.<sup>48</sup> Presence of SA in nanofibrous matrix increases the fiber diameter and bead formation due to the increase in material content and solution viscosity. Gönen et al<sup>49</sup> reported for gelatin/SA nanofibers that higher SA concentration in the polymer solution produced nanofibers with more beads and larger diameter due to higher viscosity compared to lower SA content. The presence of beads influences the fibers' uniformity as well as their mechanical strength and porosity. A lack of beads is more important than the diameter of the nanofibers regarding drug release because the beads can trap some portion of the drug.<sup>48</sup> Although Ghitescu et al<sup>50</sup> reported that the fibers became larger with increasing drug content, as a result of difficult splitting of the droplets under the same electric field as well as noncovalent interactions between the polymer chains and the drug. Contrarily, incorporation of verapamil HCl into the PVA-SA blend did not create a difference in fiber diameter.

For composite PVA-Z nanofibers (Z4) the high volatility of ethanol changed the morphology of the placebo composite fibers and weakened the possibility of bead formation. In contrast to pure PVA (N0) and PVA-SA (N2) electrospun fibers, ethanol is more volatile than water which caused an increase in the concentration of PVA-Z polymer blend. It is known that polymer solutions of higher concentration generally show more stress relaxation times which favor the production of nanofibers characterized by less bead formation and improved morphology.<sup>51</sup> In contrast to PVA-SA composite nanofibers; the decrease in the average diameter of the composite nanofibers (PVA-Z) with the inclusion of verapamil HCl (Z5) highlights that the drug's influence on fiber diameter varies depending on the polymer blend and solvent used. The reduced fiber diameter of verapamil HCl-loaded PVA-Z nanofibers can be explained in terms of the improved solution electrospinning properties which could be attributed to the presence of verapamil HCl in the polymer solution acting as a plasticizer.<sup>52</sup> Similarly, Motealleh et al<sup>53</sup> reported that the addition of chamomile slightly decreases the average diameter of the electrospun mats from 268 to 175 nm because chamomile has a plasticizing role on the polymeric chains.

The electrospinning technique is extremely sensitive to the number of charge carriers in the electrospinning solution. The presence of ions of verapamil HCl in the alcohol solution gave rise to a higher electric charge density on the jet surface during electrospinning. Thus, higher elongation forces are then imposed under the influence of the electrical field as a result of self-repulsion between the additional charges on the electric jet. As a result, beads become more spindle like leading to the small diameter of the final nanofibers. As well as the charge density, the size of the ions has a significant influence on the fiber diameter. Ions with a smaller atomic radius exhibit higher charge capacity and accordingly a higher mobility under the effect of the external electric field.<sup>54</sup> In the current study, chloride ions in verapamil HCl have a small radius. Therefore, the electrospun fibers from the PVA-Z, verapamil HCl solution possessed a small average fiber diameter. Johnson et al<sup>55</sup> demonstrated that the inclusion of a drug may reduce the nanofiber diameter if it leads to an increase in the number of charge carriers in the polymer solution as a result of the increase in coulombic repulsion and in turn increase in the stretching force applied to the ejected jet. Consequently, high stretching force for a longer time reduces the final diameter of the fiber.<sup>56</sup>

Moreover, verapamil HCl in ethanol may result in increased polarity as well as enhanced conductivity of the electrospinning solution which in turn causes a decrease in fiber diameter. This hypothesis was in agreement with Toncheva et al<sup>57</sup> who reported that the electrospinning of solutions of higher conductivity gave rise to the fabrication of

nanofibers with a relatively smaller average diameter. Solutions with high conductivity possess higher charge-carrying capacities, resulting in high elongation forces applied on the jet which in turn causes a decrease in diameter.

These findings suggested that the difference in the type of blended polymers, and solvent system composition play a significant role in determining fiber morphology, average diameter as well as maximum loaded drug amount. This might be due to the fact that each polymer blend has its own physical properties which greatly control the amount of encapsulated drug.

FTIR spectra verified intermolecular hydrogen bonding between SA and PVA which reduces the repulsive forces among polyanionic SA chains, and thus allowing for successful electrospinning of PVA-SA blends.<sup>42,43</sup> Similarly, verapamil HCl, PVA and zein have amino groups or free hydroxyl groups that act as proton donors, in addition carbonyl groups that serve as proton receptors for hydrogen bonding. Consequently, hydrogen bonding can be expected to exist.<sup>58</sup> This explains why most of the peaks of verapamil HCl, PVA, and zein in the PVA-Z drug-loaded nanofibers (Z5) have been overlapped and shifted suggesting hydrogen bond formation and compatibility of components with no chemical interaction.

Hydrogen bond interaction between the drug and the blended polymers also explains the obtained high EE%. Lack of drug aggregates on the fiber surface implies no phase separation during electrospinning. Due to the good drug solubility in the polymer blends; the entrapped drug was dispersed in the fiber matrix, which is important to avoid unfavorable drug release pattern, leading to high quality nanofibers.

Generally, in electrospun nanofibers where the drug is dissolved in the polymer solution prior to electrospinning, the release profile in an aqueous environment is biphasic with an initial burst release phase followed by a much slower second phase. The burst release can be attributed mainly to the small diameter and the high surface area of the nanofibers which guarantee short diffusion pathways and are favorable to mass transfer of the drug.<sup>59</sup> The slower drug release from PVA-Z composite nanofibers is most probably due to the lower solubility of zein in phosphate buffer pH 7.4 compared to that of SA owing to its hydrophobic nature which enables it to control the release of the entrapped drugs.<sup>60</sup> However, drug release could not reach 100% in both PVA-SA and PVA-Z composite nanofibers, which may be due to the design of the release experiment to mimic the actual way of in vivo application. This design led to hydration and swelling of the nanofibrous mats inside the cups that hindered the complete release of the drug in the release medium.

Regarding wound healing results, all composite nanofiber mats produced decrease in wound exudate, congestion relief, and recovery with no cellular reaction or scar formation. Comparing verapamil HCl-loaded nanofibers with conventional verapamil HCl gel, results showed obvious superiority of verapamil HCl-loaded nanofibers despite the small verapamil HCl dose. The nonsignificant difference between verapamil HCl gel and control groups ( $p=0.814$ ) could be attributed to insufficient dose of verapamil HCl in the conventional gel to affect the healing process. The superior efficacy of the placebo PVA-SA (N2) compared with the placebo PVA-Z (Z4) could be explained the inherent wound healing potential of SA. SA can effectively absorb wound exudates and provide the environment suitable for rapid granulation and re-epithelialization.<sup>14</sup>

Verapamil HCl-loaded PVA-SA (N6) and PVA-Z (Z5) nanofibers both achieved complete healing by the end of experiment due to the unique properties of nanofibers such as, large specific surface to volume ratio, porous structure that allows drainage of the wound exudates and permeation of atmospheric oxygen to the wound. This is in addition to superior mechanical performance, and similarity between the nanofibrous structure and the extracellular matrix (ECM).<sup>61</sup> The faster percentage of wound closure afforded by verapamil HCl-loaded PVA-SA nanofibers (N6) over PVA-Z composite nanofibers (Z5) which was evident during the first week of treatment could be attributed in part to the slower solubility and drug release rate of PVA-Z nanofibers and the pH of wound exudate as previously verified by the release experiment. In addition, it could be attributed to the ability of SA to provide a moist environment optimum for wound healing.<sup>14</sup> However, by the end of treatment both nanofiber formulations achieved complete healing with histological characteristic superiority of verapamil HCl-loaded PVA-Z nanofibers (Z5) despite its more delayed percentage of wound closure relative to verapamil HCl-loaded PVA-SA nanofibers (N6). These results agreed with that reported by Ghalei et al<sup>61</sup> where zein can provide cells with a recognizable, physiologically relevant platform to proliferate and ultimately remodel. Natural polymers usually contain specific molecular domains that can support and guide cells at various stages of their development. They can thus enhance biological interaction of the dressing with the host tissue. The increased cell



proliferation in zein containing dressings during the second week indicates the ability of zein as a natural polymer containing biocompatible amino acids to promote fibroblast proliferation. The combination of hydrophobic zein with hydrophilic PVA in the nanofibrous mat led to better cellular proliferation and spreading.

Scars might appear as hypertrophic deformity or impaired pigmentation of the healed wound after epithelialization.<sup>62</sup> Several steps occur in the wound healing processes, such as clotting, inflammation, collagen deposition, granulation, shrinkage of wound, and re-epithelization. Impairment of any of these processes leads to undue scar formation. Although evaluation of scar development seems necessary, this is still a neglected area, and yet there is no agreement on the best method for scar assessment. In the current study, despite the low verapamil HCl dose, absence of scars in all wounds treated with the developed nanofibrous mats (N6 and Z5) was observed. This result agreed with Boggio et al<sup>33</sup> who reported that verapamil HCl is an effective scar modulator that prohibits the development of hypertrophic scars and keloids in the postoperative period. This effect was improved even more by incorporation into the nanofibrous structure with its unique wound healing properties preventing scar formation.

Overall, *in vivo* results indicated that the prepared nanofibrous mats combined the beneficial properties of the biopolymers and verapamil HCl as well as increasing the functionality by exploiting the unique advantages of nanofibrous mats in wound healing. Such combined unique properties of the developed composite nanofibrous mats enhanced the effectiveness of wound healing of verapamil HCl enabling it to exhibit, not only complete, but also histologically appropriate wound healing at a small dose, which proved to be insufficient in the case of the conventional gel.

## Conclusion

Economic and environmentally friendly verapamil HCl-loaded composite nanofibrous mats have been successfully developed from the two biopolymers: sodium alginate polysaccharide of marine origin (brown algae) and zein protein from plant origin (corn or maize). Verapamil HCl is usually used for scar modulation after scar formation either topically or by intralesional injection. However, the formulation of verapamil HCl as nanofibers either using PVA-SA or PVA-Z blends for the purpose of wound healing without scar formation was considered a novelty that has not been presented in the literature so far. By controlling the electrospinning parameters, polymer blend composition and drug load; uniform and continuous verapamil HCl-loaded composite nanofibrous mats in the nano-range diameter were effectively fabricated. The mats used throughout the current study were not fragile, contrarily they offered durability, ease of handling and manageability. Both verapamil HCl-loaded composite nanofibrous mats have produced complete healing with no scar formation. Although verapamil HCl-loaded PVA-SA nanofibers provided a faster healing rate than PVA-Z nanofibers, the latter demonstrated more sustained drug release and superiority in enhancing the histological characteristics of the newly formed tissues than PVA-SA nanofibers. These results suggest the possible therapeutic benefits that could be obtained by combining the two types of drug-loaded composite nanofibrous mats (PVA-SA and PVA-Z) together in one smart multilayered wound dressing to provide an efficient platform for adequate wound healing with no scar formation.

## Limitations and Future Research

The current study, like any other, had some limitations. First, incorporation of higher biopolymer or drug loads was not possible. However, by the end of the *in vivo* study period, both verapamil HCl-loaded composite nanofibrous mats have produced complete healing with no scar formation. Second, the data of the mechanical testing were not presented, and selection of the formulations was based on the durability and ease of handling of the mats. Regarding the *in vivo* testing, using three rats only in each treatment group with the four wounds all coming from the same rat necessitated the authors to perform complex statistical analysis to avoid violation of the independence of observations assumption. Finally, the wound healing efficacy was studied for each type of the composite nanofibrous mats separately while the efficacy of the two types when combined was not examined. Therefore, the authors recommend more detailed *in vitro*, and *in vivo* studies to be conducted in the future using larger sample sizes. In addition, the wound healing efficacy on other types of wounds such as chronic wounds or pressure ulcers can be tested for each type of the composite nanofibrous mats separately and when combined together in one smart dressing.

## Ethics Approval

All institutional and national guidelines for the care and use of laboratory animals were followed. Experimental protocol was approved by Institutional Animal Care and Use Committee, Faculty of Pharmacy, Alexandria University. Animal experiments were performed in accordance with UK Animals (Scientific Procedures) Act, 1986 and EU Directive 2010/63/EU guidelines for the use of experimental animals.

## Acknowledgment

The authors wish to acknowledge Assistant Professor Wessam M. El Refaie, Department of Pharmaceutics, Faculty of Pharmacy, Pharos University, Alexandria, Egypt, for her great help in the animal study. The authors also wish to acknowledge the Department of Histology and Cell Biology, Faculty of Medicine, Alexandria University, Alexandria, Egypt, for their help in the histological interpretation.

## Author Contributions

All authors made a significant contribution to the work reported; whether in the conception, study design, execution, acquisition of data, analysis and interpretation or in all these areas; took part in drafting, revising, or critically reviewing the article; gave final approval of the version to be published; have agreed on the journal to which the article has been submitted; and agree to be accountable for all aspects of the work.

## Funding

The authors declare that this research did not receive any specific fund or grant from funding agencies in the public, commercial, or not-for-profit sectors.

## Disclosure

The authors declare that they have no relevant financial or non-financial conflict of interests to disclose.

## References

1. Smith R, Russo J, Fiegel J, Brogden N. Antibiotic delivery strategies to treat skin infections when innate antimicrobial defense fails. *Antibiotics*. 2020;9:56.
2. Dong Y, Zheng Y, Zhang K, et al. Electrospun nanofibrous materials for wound healing. *Adv Fiber Mater*. 2020;2:212–227. doi:10.1007/s42765-020-00034-y
3. Azimi B, Maleki H, Zavagna L, et al. Bio-based electrospun fibers for wound healing. *J Funct Biomater*. 2020;11:67. doi:10.3390/jfb11030067
4. Taemeh MA, Shiravandi A, Korayem MA, Daemi H. Fabrication challenges and trends in biomedical applications of alginate electrospun nanofibers. *Carbohydr Polym*. 2020;15(228):115419. doi:10.1016/j.carbpol.2019.115419
5. Ji Y, Song W, Xu L, Yu DG, Bligh SWA. A review on electrospun poly(amino acid) nanofibers and their applications of hemostasis and wound healing. *Biomolecules*. 2022;12:794. doi:10.3390/biom12060794
6. Xue J, Xie J, Liu W, Xia Y. Electrospun nanofibers: new concepts, materials, and applications. *Acc Chem Res*. 2017;50(8):1976–1987. doi:10.1021/acs.accounts.7b00218
7. Zhou Y, Wang M, Yan C, Liu H, Yu DG. Advances in the application of electrospun drug-loaded nanofibers in the treatment of oral ulcers. *Biomolecules*. 2022;12:1254. doi:10.3390/biom12091254
8. Liu Y, Chen X, Liu Y, Gao Y, Liu P. Electrospun coaxial fibers to optimize the release of poorly water-soluble drug. *Polymers*. 2022;14(3):469.
9. Lv H, Yu DG, Wang M, Ning T. Nanofabrication of janus fibers through side-by-side electrospinning - a mini review. *Mater Highlight*. 2021;2(1–2):18. doi:10.2991/math.k.210212.001
10. Ghosal K, Augustine R, Zaszczynska A, et al. Novel drug delivery systems based on triaxial electrospinning based nanofibers. *React Funct Polym*. 2021;1(163):104895. doi:10.1016/j.reactfunctpolym.2021.104895
11. Nagiah N, Murdock CJ, Bhattacharjee M, Nair L, Laurencin CT. Development of tripolymeric triaxial electrospun fibrous matrices for dual drug delivery applications. *Sci Rep*. 2020;10(1). doi:10.1038/s41598-020-57412-0
12. Datta LP, Manchineella S, Govindaraju T. Biomolecules-derived biomaterials. *Biomaterials*. 2020;230:119633. doi:10.1016/j.biomaterials.2019.119633
13. Zhang B, Yan X, He HW, Yu M, Ning X, Long YZ. Solvent-free electrospinning: opportunities and challenges. *Polym Chem*. 2017;8:333. doi:10.1039/C6PY01898J
14. Fu R, Li C, Yu C, et al. A novel electrospun membrane based on moxifloxacin hydrochloride/poly(vinyl alcohol)/ sodium alginate for antibacterial wound dressings in practical application. *Drug Deliv*. 2016;23(3):818–829. doi:10.3109/10717544.2014.918676
15. Sun F, Guo J, Liu Y, Yu Y. Preparation, characterizations and properties of sodium alginate grafted acrylonitrile/polyethylene glycol electrospun nanofibers. *Int J Biol Macromol*. 2019;137:420–425. doi:10.1016/j.ijbiomac.2019.06.185
16. Fang D, Liu Y, Jiang S, Nie J, Ma G. Effect of intermolecular interaction on electrospinning of sodium alginate. *Carbohydr Polym*. 2011;85(1):276–279.



17. Wongkanya R, Chuysinuan P, Pengsuk C, et al. Electrospinning of alginate/soy protein isolated nanofibers and their release characteristics for biomedical applications. *J Sci Adv Mater Dev.* 2017;2(3):309–316.
18. Teboho M, Jacobs N, Adriaan L. Electrospun alginate nanofibres as potential bio-sorption agent of heavy metals in water treatment. *Express Polym Lett.* 2017;11:652–663. doi:10.3144/expresspolymlett.2017.63
19. Viganì B, Rossi S, Milanese G, et al. Electrospun alginate fibers: mixing of two different poly(ethylene oxide) grades to improve fiber functional properties. *Nanomaterials.* 2018;8(12):971. doi:10.3390/nano8120971
20. Li W, Li X, Chen Y, et al. Poly(vinyl alcohol)/sodium alginate/layered silicate based nanofibrous mats for bacterial inhibition. *Carbohydr Polym.* 2013;92(2):2232–2238. doi:10.1016/j.carbpol.2012.12.004
21. Labib G. Overview on zein protein: a promising pharmaceutical excipient in drug delivery systems and tissue engineering. *Expert Opin Drug Deliv.* 2018;15(1):65–75. doi:10.1080/17425247.2017.1349752
22. Fan X, Wang Y, Zheng M, et al. Morphology engineering of protein fabrics for advanced and sustainable filtration †. *J Mater Chem A.* 2018;6:21585–21595. doi:10.1039/C8TA08717B
23. Singh N, Georget DM, Belton PS, Barker SA. Zein-iodine complex studied by FTIR spectroscopy and dielectric and dynamic rheometry in films and precipitates. *J Agric Food Chem.* 2009;57(10):4334–4341. doi:10.1021/jf900436q
24. Dashdorj U, Reyes MK, Unnithan AR, et al. Fabrication and characterization of electrospun zein/Ag nanocomposite mats for wound dressing applications. *Int J Biol Macromol.* 2015;1(80):1–7. doi:10.1016/j.ijbiomac.2015.06.026
25. Wang Y, Padua GW. Nanoscale characterization of zein self-assembly. *Langmuir.* 2012;28(5):2429–2435. doi:10.1021/la204204j
26. Miyoshi T, Toyohara K, Minematsu H. Preparation of ultrafine fibrous zein membranes via electrospinning. *Polym Int.* 2005;54:1187–1190. doi:10.1002/pi.1829
27. Kanjanapongkul K, Wongsasulak S, Yoovidhya T. Investigation and prevention of clogging during electrospinning of zein solution. *J Appl Polym Sci.* 2010;118:1821–1829.
28. Vogt L, Liverani L, Roether JA, Boccaccini AR. Electrospun zein fibers incorporating poly(glycerol sebacate) for soft tissue engineering. *Nanomaterials.* 2018;8(3):150. doi:10.3390/nano8030150
29. Akhmetova A, Lanno GM, Kogermann K, Malmsten M, Rades T, Heinz A. Highly elastic and water stable zein microfibers as a potential drug delivery system for wound healing. *Pharmaceutics.* 2020;12(5):458. doi:10.3390/pharmaceutics12050458
30. Sotiropoulou G, Zingkou E, Pampalakis G. Redirecting drug repositioning to discover innovative cosmeceuticals. *Exp Dermatol.* 2021;30:628–644. doi:10.1111/exd.14299
31. Spampinato SF, Caruso GI, de Pasquale R, Sortino MA, Merlo S. The treatment of impaired wound healing in diabetes: looking among old drugs. *Pharmaceutics.* 2020;13(4). doi:10.3390/ph13040060
32. Pillaiyar T, Meenakshisundaram S, Manickam M, Sankaranarayanan M. A medicinal chemistry perspective of drug repositioning: recent advances and challenges in drug discovery. *Eur J Med Chem.* 2020;1(195):112275. doi:10.1016/j.ejmech.2020.112275
33. Boggio RF, Boggio LF, Galvão BL, Machado-Santelli GM. Topical verapamil as a scar modulator. *Aesthetic Plast Surg.* 2014;38(5):968–975. doi:10.1007/s00266-014-0400-9
34. Yoshida MI, Cassiana E, Gomes L, et al. Thermal analysis applied to verapamil hydrochloride characterization in pharmaceutical formulations. *Molecules.* 2010;15:2439–2452. doi:10.3390/molecules15042439
35. Priya KS, Gnanamani A, Radhakrishnan N, Babu M. Healing potential of Datura alba on burn wounds in albino rats. *J Ethnopharmacol.* 2002;83(3):193–199. doi:10.1016/S0378-8741(02)00195-2
36. El-Refai WM, Elnaggar YS, El-Massik MA, Abdallah OY. Novel curcumin-loaded gel-core hyalurosomes with promising burn-wound healing potential: development, in-vitro appraisal and in-vivo studies. *Int J Pharm.* 2015;486(1–2):88–98. doi:10.1016/j.ijpharm.2015.03.052
37. Gong C, Wu Q, Wang Y, et al. A biodegradable hydrogel system containing curcumin encapsulated in micelles for cutaneous wound healing. *Biomaterials.* 2013;34(27):6377–6387. doi:10.1016/j.biomaterials.2013.05.005
38. Hothorn T, Hornik K, Wien W, van de Wiel MA, Zeileis A. Implementing a class of permutation tests: the coin package. *J Stat Softw.* 2008;28(8):1–23. doi:10.18637/jss.v028.i08
39. Shalumon KT, Anulekha KH, Nair SV, Chennazhi KP, Jayakumar R. Sodium alginate/poly(vinyl alcohol)/nano ZnO composite nanofibers for antibacterial wound dressings. *Int J Biol Macromol.* 2011;49(3):247–254. doi:10.1016/j.ijbiomac.2011.04.005
40. Nie H, He A, Zheng J, Xu S, Li J, Han CC. Effects of chain conformation and entanglement on the electrospinning of pure alginate. *Biomacromolecules.* 2008;9(5):1362–1365. doi:10.1021/bm701349j
41. Fong H, Chun I, Reneker DH. Beaded nanofibers formed during electrospinning. *Polymer.* 1999;40(16):4585–4592. doi:10.1016/S0032-3861(99)00068-3
42. Islam MS, Karim MR. Fabrication and characterization of poly(vinyl alcohol)/alginate blend nanofibers by electrospinning method. *Colloids Surf a Physicochem Eng.* 2010;366(1–3):135–140. doi:10.1016/j.colsurfa.2010.05.038
43. Kataria K, Gupta A, Rath G, Mathur RB, Dhakate SR. In vivo wound healing performance of drug loaded electrospun composite nanofibers transdermal patch. *Int J Pharm.* 2014;469(1):102–110. doi:10.1016/j.ijpharm.2014.04.047
44. Zhang M, Liu Y, Yi H, Luan J, Zhang Y. Electrospun zein/PVA fibrous mats as three-dimensional surface for embryonic stem cell culture. *J Text Inst.* 2014;105(3):246–255. doi:10.1080/00405000.2013.835902
45. Liu FX, Liu YJ, Cai HL, Luan JS, Zhang M. Preparation and mechanical properties of zein/PVA nanofibrous membranes. *Adv Mater Res.* 2012;466:391–395.
46. Lin J, Li C, Zhao Y, Hu J, Zhang LM. Co-electrospun nanofibrous membranes of collagen and zein for wound healing. *ACS Appl Mater Interfaces.* 2012;4(2):1050–1057. doi:10.1021/am201669z
47. Wang X, Mousavi S. Encapsulation of Lidocaine into Zein Nanofibers; 2018.
48. Diedericks H. C release of an antimicrobial substance from polymeric matrices. Controlled release of antimicrobial substances from polymer matrices. European Patent Office Publ. of Application with search report EP20040386006; 2016.
49. Gönen S, Taygun ME, Küçükbayrak S. Evaluation of the factors influencing the resultant diameter of the electrospun gelatin/sodium alginate nanofibers via Box-Behnken design. *Mater Sci Eng C Mater Biol Appl.* 2016;58:709–723. doi:10.1016/j.msec.2015.09.024
50. Ghitescu RE, Popa AM, Popa VI, Rossi RM, Fortunato G. Encapsulation of polyphenols into pHEMA e-spun fibers and determination of their antioxidant activities. *Int J Pharm.* 2015;494(1):278–287. doi:10.1016/j.ijpharm.2015.08.020

51. Song TY, Yao C, Li XS. Electrospinning of zein/chitosan composite fibrous membranes. *Chinese J Polym Sci.* 2010;28:171–179. doi:10.1007/s10118-010-8239-2
52. de Oliveira Mori CLS, Dos Passos NA, Oliveira JE, et al. Electrospinning of zein/tannin bio-nanofibers. *Ind Crops Prod.* 2014;52:298–304. doi:10.1016/j.indcrop.2013.10.047
53. Motealleh B, Zahedi P, Rezaeian I, Moghimi M, Abdolghaffari AH, Zarandi MA. Morphology, drug release, antibacterial, cell proliferation, and histology studies of chamomile-loaded wound dressing mats based on electrospun nanofibrous poly(E-caprolactone)/polystyrene blends. *J Biomed Mater Res Part B Appl Biomater.* 2013;102:977–987. doi:10.1002/jbm.b.33078
54. Zong X, Kim K, Fang D, Ran S, Hsiao BS, Chu B. Structure and process relationship of electrospun bioabsorbable nanofiber membranes. *Polymer.* 2002;43(16):4403–4412. doi:10.1016/S0032-3861(02)00275-6
55. Johnson CDL, D'amato AR, Gilbert RJ. Electrospun fibers for drug delivery after spinal cord injury and the effects of drug incorporation on fiber properties. *Cells Tissues Organs.* 2016;202(1–2):116–135. doi:10.1159/000446621
56. Bao J, Lv W, Sun Y, Deng Y. Electrospun antimicrobial microfibrillar scaffold for annulus fibrosus tissue engineering. *J Mater Sci.* 2013;48:4223–4232. doi:10.1007/s10853-013-7235-7
57. Toncheva A, Paneva D, Manolova N, Rashkov I. Electrospun poly(L-lactide) membranes containing a single drug or multiple drug system for antimicrobial wound dressings. *Macromol Res.* 2011;19(12):1310–1319. doi:10.1007/s13233-011-1206-0
58. Huang W, Zou T, Li S, Jing J, Xia X, Liu X. Drug-loaded zein nanofibers prepared using a modified coaxial electrospinning process. *AAPS PharmSciTech.* 2013;14(2):675–681. doi:10.1208/s12249-013-9953-1
59. Kyzioł A, Michna J, Moreno I, Gamez E, Irusta S. Preparation and characterization of electrospun alginate nanofibers loaded with ciprofloxacin hydrochloride. *Eur Polym J.* 2017;1(96):350–360. doi:10.1016/j.eurpolymj.2017.09.020
60. Shukla R, Cheryan M. Zein: the industrial protein from corn. *Ind Crops Prod.* 2001;13(3):171–192. doi:10.1016/S0926-6690(00)00064-9
61. Ghalei S, Asadi H, Ghalei B, Ghalei S. Zein nanoparticle-embedded electrospun PVA nanofibers as wound dressing for topical delivery of anti-inflammatory diclofenac. *J Appl Polym Sci.* 2018;135:46643. doi:10.1002/app.46643
62. Idriss N, Maibach HI. Scar assessment scales: a dermatologic overview. *Skin Res Technol.* 2009;15:1–5. doi:10.1111/j.1600-0846.2008.00327.x

## Drug Design, Development and Therapy

Dovepress

### Publish your work in this journal

Drug Design, Development and Therapy is an international, peer-reviewed open-access journal that spans the spectrum of drug design and development through to clinical applications. Clinical outcomes, patient safety, and programs for the development and effective, safe, and sustained use of medicines are a feature of the journal, which has also been accepted for indexing on PubMed Central. The manuscript management system is completely online and includes a very quick and fair peer-review system, which is all easy to use. Visit <http://www.dovepress.com/testimonials.php> to read real quotes from published authors.

Submit your manuscript here: <https://www.dovepress.com/drug-design-development-and-therapy-journal>